The 8th International Supercritical $CO_2$ Power Cycles Symposium
February 27-29th, 2024, San Antonio, TX
Paper #25

# Multi-Model Predictive Control for Enhanced Load Following of a $sCO_2$ Recompression Brayton Cycle

Jacob Albright[1,2]
Chemical Engineer
National Energy Technology Laboratory
Morgantown, WV

Eric Liese[1]
Mechanical Engineer
National Energy Technology Laboratory
Morgantown, WV

***[1]National Energy Technology Laboratory, 3610 Collins Ferry Road, Morgantown, WV 26507, USA***
***[2]NETL Support Contractor, 3610 Collins Ferry Road, Morgantown, WV 26507, USA***

*Jacob Albright has worked at the National Energy Technology Laboratory (NETL) for 7 years performing work in the areas of dynamic modelling and process control. He has worked as a research engineer under Leidos at NETL for the past 2 years. He received a B.S. in Chemical Engineering from West Virginia University in 2014. He supports the development of dynamic models and control systems for $sCO_2$ projects at NETL in the Strategic Systems Analysis & Engineering group.*

*Eric Liese is a research engineer currently doing steady state and dynamic process simulation in the Strategic Systems Analysis & Engineering division at the U.S. Department of Energy's (DOE) National Energy Technology Lab (NETL). He has been working for over 30 years in various areas of experimental and computational research for fossil fuel energy technologies, like fuel cells, gas turbines, combined cycles, and most recently supercritical CO2 systems. Mr. Liese received his B.S in Aeronautical Engineering from Purdue University and M.S. in Mechanical Engineering from West Virginia University.*

## ABSTRACT

Supercritical carbon dioxide recompression Brayton cycles (sCO2 RCBC) are a promising alternative to traditional steam cycles. However, increasing renewables penetration to the grid will require fast load ramping of any new non-baseload power systems. This will require considerations to the controls architecture to ensure safe and efficient operation of this novel power cycle. While traditional controls, namely PI and PID, can sufficiently operate the system, further improvements to the cycle response while still maintaining high cycle efficiency will require the consideration of advanced control methods. This paper presents the application of a linear multi-model predictive controller (L-MMPC) for use as a substitute to the standard inventory management controller (IMC). Discussions on the control scheme utilized and the improvements to the load response time and tracking are included.

## INTRODUCTION

Supercritical $CO_2$ ($sCO_2$) driven power cycles are becoming increasingly promising as an alternative to traditional steam-based power generation. As the world moves towards a net-zero carbon future, high-efficiency power systems will become increasingly necessary for both existing fossil fuel generation, to reduce carbon emissions, as well as for new renewable energy to increase cost effectiveness. Several projects are currently underway, including the Supercritical Transformational Electric Power (STEP) pilot plant. This is a U.S. Department of Energy based project to build and test both a simple Brayton cycle as well as recompression Brayton cycle (RCBC) for the purpose of stress testing the new technology and determine the capabilities of the advanced cycle [1-3]. The STEP team has recently commissioned the cycle and is planning to begin operation in early 2024 [4].

Control of this process has been examined in Liese et al. [5] and was continued in Albright et al. [6]. In both works, sufficient control is achieved to operate across the entire operational range, i.e. from 10 to 4MW. The load tracking response demonstrated by these works is acceptable and follows the demand profile closely but typically has a long approach to the final setpoint (SP). Due to operation near the critical region of $CO_2$, caution must be taken when operating the system aggressively. The control action of specific controllers must be limited to avoid instabilities in the process. The result of this limitation is fast load tracking during ramps but a somewhat long settling time towards the end of a given ramp. In order to further improve the response of this process to fast ramps in load, an advanced control method is considered.

This work uses a linear time-invariant (LTI) multi-model predictive controller (MMPC) to improve the load tracking response of the RCBC. By replacing the primary load controller with the MMPC, fast tracking can still be achieved while simultaneously improving the approach to the final SP. The MMPC implementation is provided and the preliminary results for a full turndown and partial turn-up response are given.

## PROCESS MODEL & CONTROLS

The process flow diagram for the $sCO_2$ RCBC used for this test is given in Figs. 1A and 1B. A more detailed explanation of the models and software used can be found in Liese et al. [5]. A brief summary of the cycle is given below.

The $sCO_2$ RCBC is an indirect heat, gas fired, power cycle. The heat generated from the combustor is transferred to the cycle from the primary heater (PHX). The $sCO_2$ is heated to approximately 715°C and then expanded in the turbine (TRB). The turbine exhaust is sent through the high temperature recuperator (HTR) to preheat the feed to the PHX. The $sCO_2$ is then sent through the low temperature recuperator (LTR) for further heat recuperation. The flow is then split into two streams that go to the main compressor (MC) and the bypass compressor (BC). The portion of the $sCO_2$ flow that is sent to the MC is pre-cooled in the main cooler which is water cooled. This system (CoolSys) is shown separately in Fig 1B. The $sCO_2$ cycle inventory is maintained by manipulating inlet and outlet control valves to the inventory storage tank (IST).

Previous control methods applied to this system are given in Liese et al. [4] and Albright et al. [5]. The main control architecture used in those studies is maintained for this system. There is no significant change noted for the performance of the turbine inlet temperature (TIT), the main compressor inlet temperature (MCIT), or the surge controllers for the compressors. All controllers not mentioned specifically use the standard form of the PID and have been manually tuned to achieve an acceptable response.

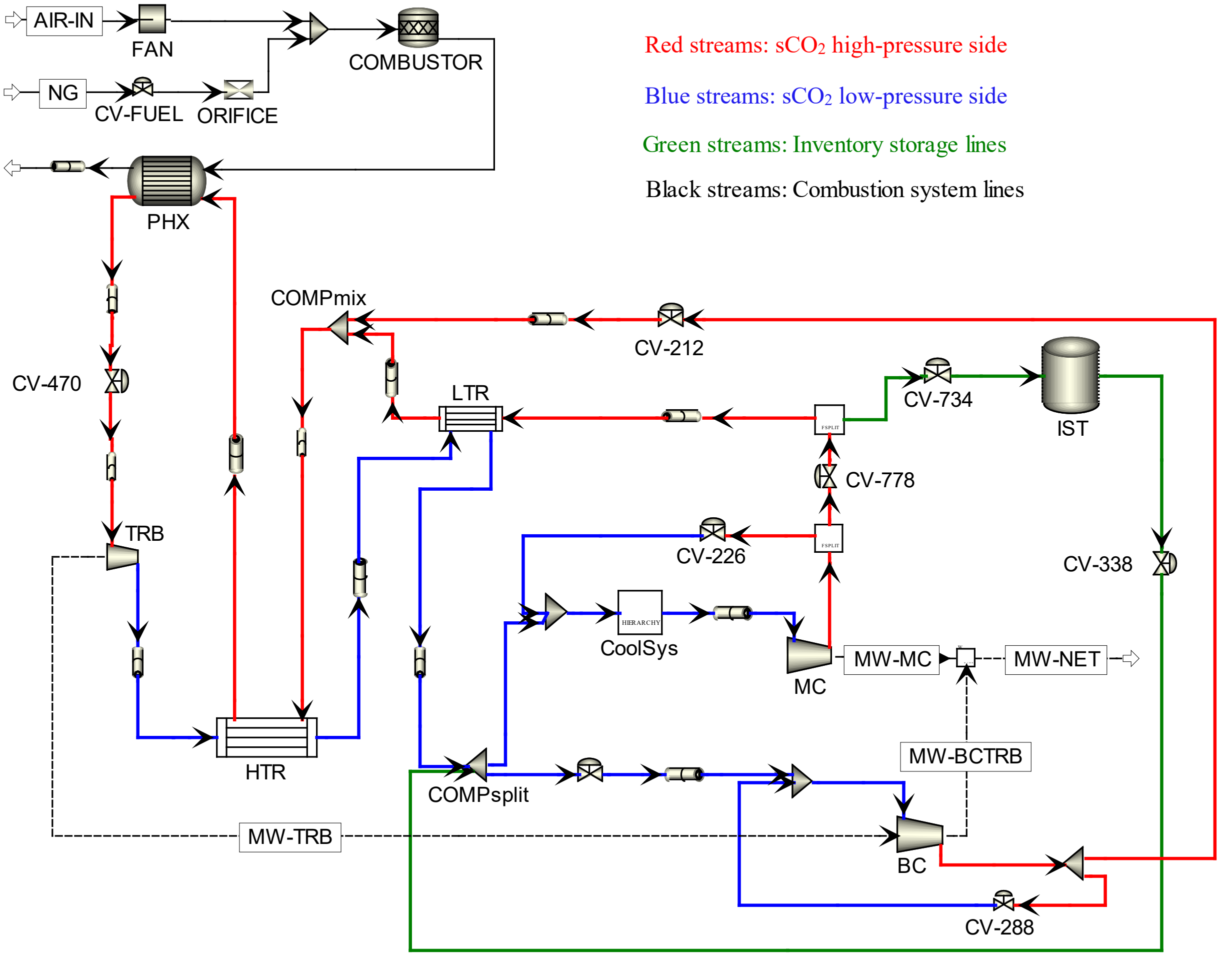

Figure 1A Process flow diagram of the recompression closed Brayton cycle.

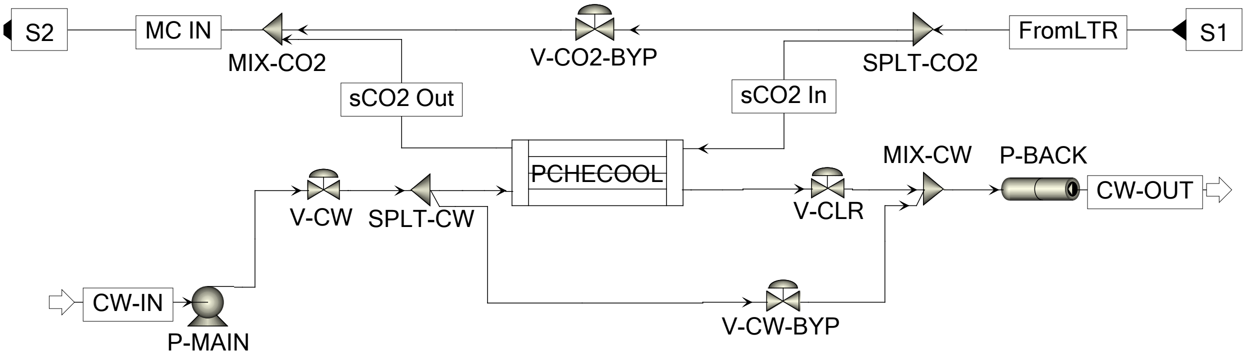

Figure 1B Process flow diagram of the main cooler system

This study focuses on the changes to the inventory management control (IMC). Figure 2 shows the control diagram of the IMC. A main load controller (MWC) receives a load setpoint (SP) and then sends an output signal to the pressure controller (PC) for the IST. A split range controller manipulates the tank inlet valve (CV-734) and outlet valve (CV-338) in order to remove and introduce $sCO_2$ inventory from/to the cycle, respectively.

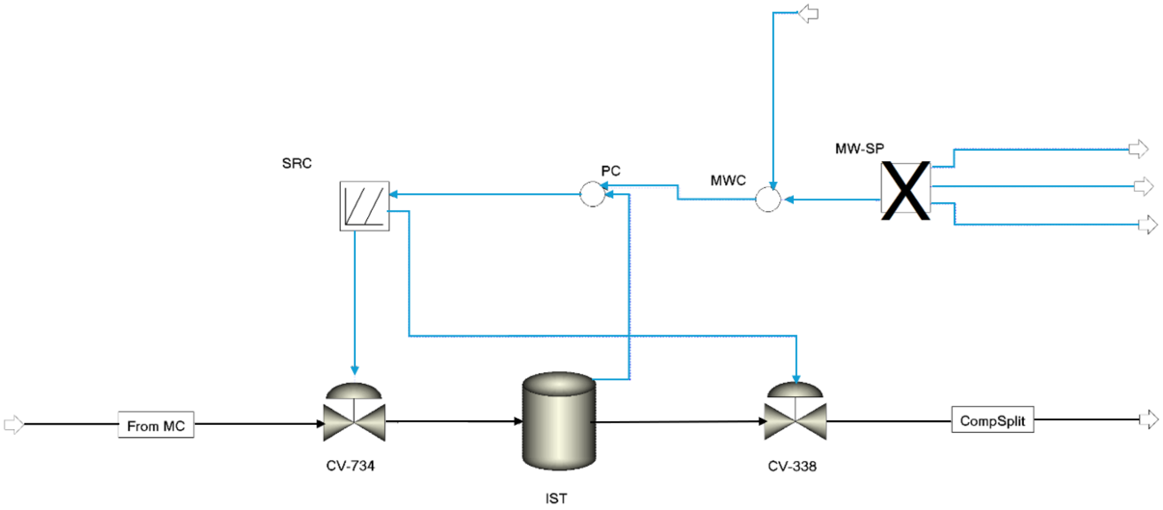

**Figure 2.** Inventory management control with cascaded pressure control.

The IMC primary controller, MWC, that adjusts the secondary IST pressure controller SP has been replaced with a model predictive controller (MPC). This MPC uses a linear time-invariant representation of the dynamic model, given in eq. (1).

$$x(k+1) = Ax(k) + Bu(k) + Ke(k) \tag{1}$$

$$y(k+1) = Cx(k) + Du(k) + e(k)$$

$$x(k), y(k), u(k), e(k) \in R^n$$

$$U_{LB} \leq u_n \leq U_{UB}$$

In eq. (1), x, u, y and e are the state, input, output and disturbance vectors, respectively. A, B, K, C and D are the state space matrices that are to be estimated to give a linear representation of the full dynamic model. The use of this type of representation allows for fast generation of the optimal input sequence which is important for this application as the system is being aggressively ramped and a fast controller response will be necessary. The optimal sequence is determined by the MPC by minimizing a cost function given in eqs. (2) and (3).

$$J(z_k) = J_y(z_k) + J_u(z_k) + J_{\Delta u}(z_k) + J_\varepsilon(z_k) \tag{2}$$

$$J_y(z_k) = \sum_{i=1}^{p} \left( \frac{w_{1,i}}{s_{1,i}} [r_1(k+i|k) - y_1(k+i|k)] \right)^2$$

(3)

In eq. (2), J represents the overall cost function, which is a sum of several terms that are all based on a QP decision, $z_k$, for the current control interval k. Eq. (3) is the expanded first term of the cost function, which is the output reference tracking function. This measures the deviation of the output, $y_i$, from reference value, $r_i$, over the current control interval. The relative impact of each cost function is determined by the weight, $w_{1,I}$, and scaling factor, $s_{1,I}$, which can be manually tuned to obtain different response characteristics from the MPC. Two other adjustable parameters can influence the performance of the MPC, namely the prediction and control horizon. The prediction horizon (PH) is the entire range over which the cost function is minimized. The control horizon (CH) determines the number of variables to optimize over, which is the number of control moves at each time instant k. Typically, PH is chosen to be much larger than CH in order to ensure a stable response as well as to reduce the computation expense associated with a larger optimization problem as the CH increases.

Each term in the overall cost function resembles eq. (3) but are tracking a different performance metric. $J_u$ penalizes the input deviation from a specified reference value while $J_{\Delta u}$ penalizes excessive input movement over the course of the control interval. $J_\varepsilon$ is the constraint violation term but only applies to the upper and lower bounds of the process variables for this implementation.

This MPC design approach is then used to split the operational range of the RCBC into 3 regions:

- 10 to 8MW, $MPC_1$
- 8 to 6MW, $MPC_2$
- 6 to 4MW, $MPC_3$

Separating the operating range into 3 sections was done as an initial point of testing for the MMPC. It is possible that more or less model segments would be optimal, but that is outside the current scope of this work. Models are generated for each section and then used to design and test a specific MPC for that section. This is done for several reasons. During regular operation, the IST pressure increases and decreases according to the load required. This also changes the driving force between the tank and the high- or low-pressure side of the cycle, depending on which valve is being operated. Additionally, the low side cycle pressure decreases during turn-down operation, moving the conditions at the inlet of the main compressor closer to the critical point. This changes the properties significantly and can alter the dynamic response of the cycle due to the impact of the main compressor performance on the overall cycle.

## RESULTS AND DISCUSSION

Figure 3 shows the data utilized for model generation in the MPC framework. Several sections of randomly generated perturbations are generated across the selected operational range of the RCBC, in this case 10 to 8MW. The MWC is not operational during this data generation period, as it is necessary to determine the output response to various input disturbances so that a sufficient representation of the cycle can be generated for the region being examined. The load SP adjusted here is only used to mimic the controller settings during normal operation, as it is used to perform gain scheduling and SP adjustment in the cooler controls and turbine exhaust gas control. By more closely representing the response of the system while other controllers are active, a better representation of the system can be obtained and therefore an improved response from the MPC in this region.

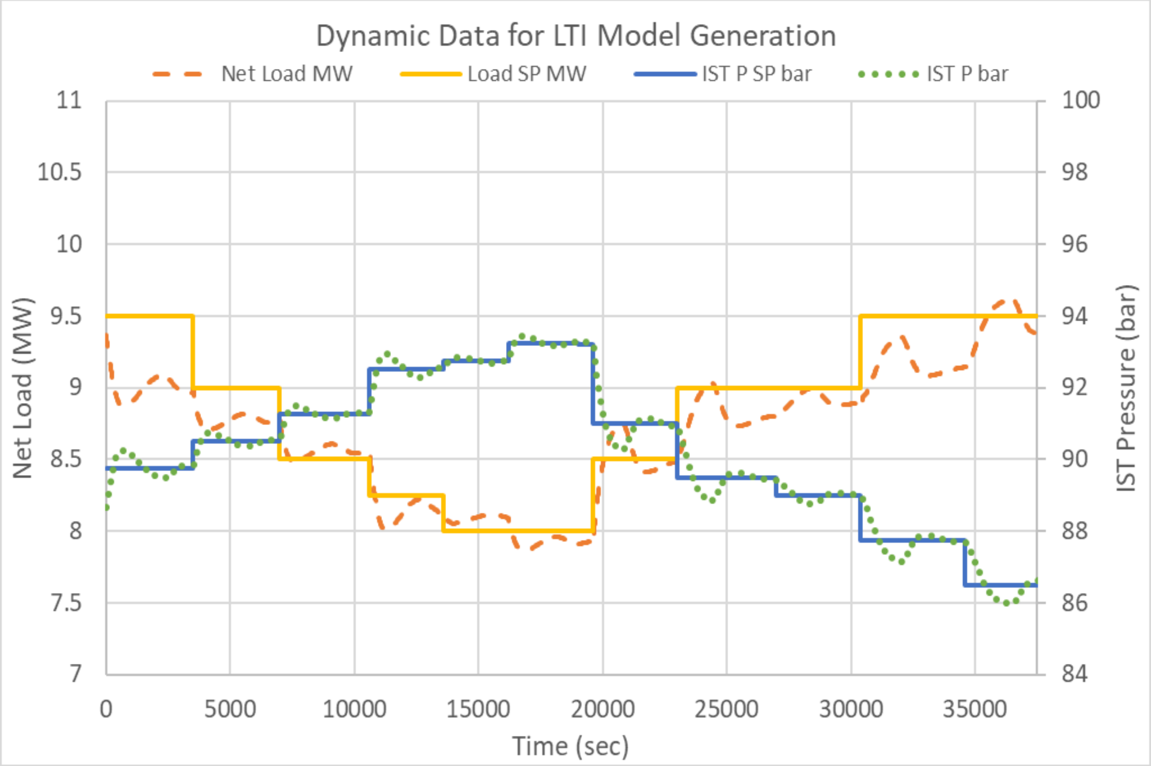

**Figure 3.** Example of data used for LTI model generation

The settings for the MPCs generated using this data are given below in Table 1. In Table 1, the PH and CH are given, as well as the weights associated with each cost function. These should not be considered optimal but were found to be sufficient for this work. The input tracking, $w_u$, and the constraint violation, $w_\varepsilon$, weights are not adjusted for these designs as their impact was not found to be significant. This is due the lack of an input reference value and few constraints imposed on the current problem. It can be seen in Table 1 that the PH is increased for each subsequent MPC design. It was found that operating closer to the minimum load of 4MW caused a decrease in the response time and that by increasing the PH there was an increase in the control action in these regions. To balance this increase in control action, the input differential weight, $w_{\Delta u}$, is increased for $MPC_2$ and $MPC_3$ to prevent excessive undershoot/overshoot at the end of a given ramp. The output tracking weight, $w_y$, is similar for each MPC to ensure minimal SP-PV difference over the course of the response.

Table 1. MPC Settings

| | PH | CH | $w_y$ | $w_u$ | $w_{\Delta u}$ | $w_\varepsilon$ |
|---|---|---|---|---|---|---|
| $MPC_1$ | 200 | 20 | 0.95 | 0.01 | 0.1 | 0.04 |
| $MPC_2$ | 1200 | 200 | 0.9 | 0.01 | 0.3 | 0.04 |
| $MPC_3$ | 3000 | 100 | 0.9 | 0.01 | 0.2 | 0.04 |

Figure 4 shows the results for the turn-down scenario of the RCBC using a 3-section MPC. As can be seen in Figure 4, the load tracks the demand SP closely for each subsequent ramp down in power. There is a small delay in response once each ramp is initiated, which can be attributed to the MPC model switching. Once a new MPC comes online, there is a short delay before the MPC responds causing a sharp increase in the initial output seen around t=60, 530, and 1100. The MPC output is somewhat aggressive, but this may be due to the way in which the IMC operates. Due to the split range control, the output from the PC must be changed quickly to operate both the inlet and outlet valve in quick succession to dampen any oscillations. Typically, only one valve is operated, inlet for turn-down and outlet for turn-up, which causes a slow first-order approach to the final demand SP as the valve slowly closes off over the course of the response. The MPC aggressively changes the pressure SP to the PC to cause a rapid shift in the output and operate both valves quickly. This results in a fast approach to the final SP with some oscillation around the final SP for each segment. Further refinement of the separate MPCs may reduce the initial undershoot but would likely increase the load tracking error or settling time.

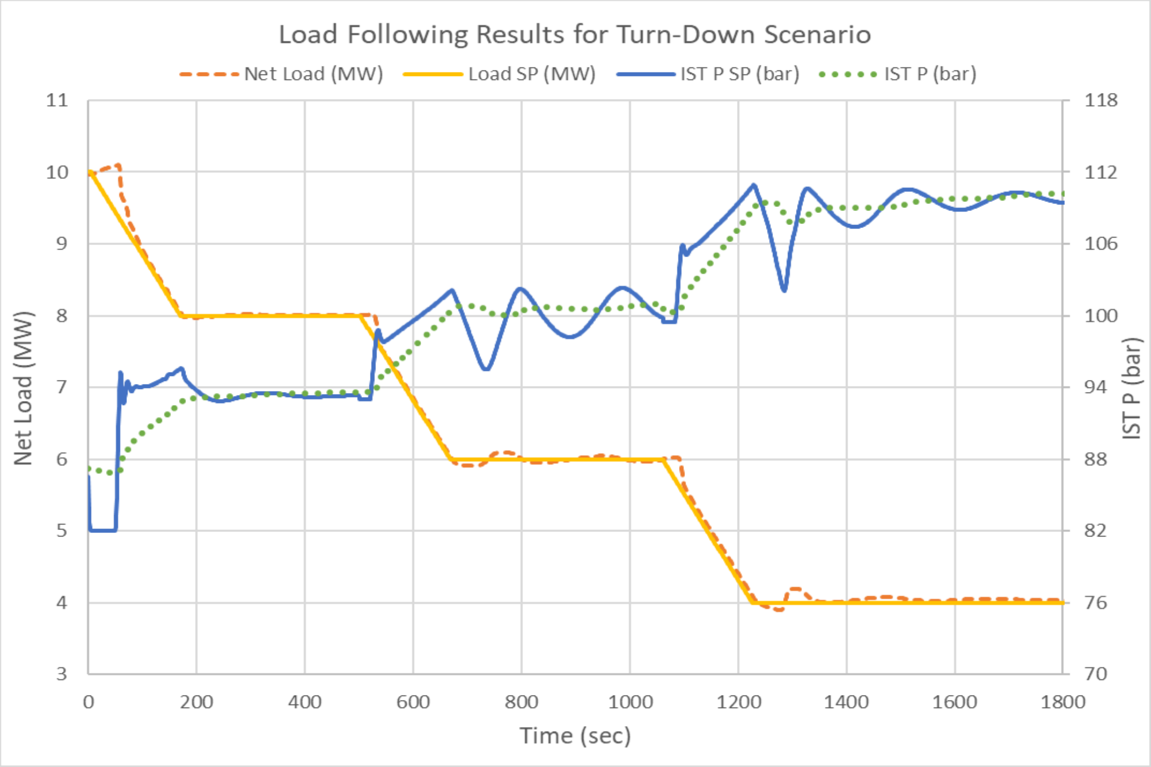

**Figure 4.** Load following response of MMPC for turndown scenario

Figure 5 shows the load following response of the RCBC for a turn-up scenario using a similar 3-section MPC. The MPCs generated for the turn-up response did not result in a similar reduction in load tracking and settling time. The MPC response is somewhat like the turn-down case but does not cause as rapid of a change in the load response. The load still meets the load SP quickly but does not settle out in a similar manner. The response from 4 to 6MW and from 6 to 8MW both have small, sustained oscillations around the final SP. It is likely that the optimizer of the MPC response could not determine the correct IST P SP to quickly settle the load response. This may mean that a separate set of MPCs for the turn-up response may be required to efficiently operate this system. Additionally, the final segment from 8 to 10MW reached a pressure pinch point between the IST P and the low pressure side of the cycle. The response was similar to the previous two ramps, however, so the rest of the approach would not be expected be significantly different.

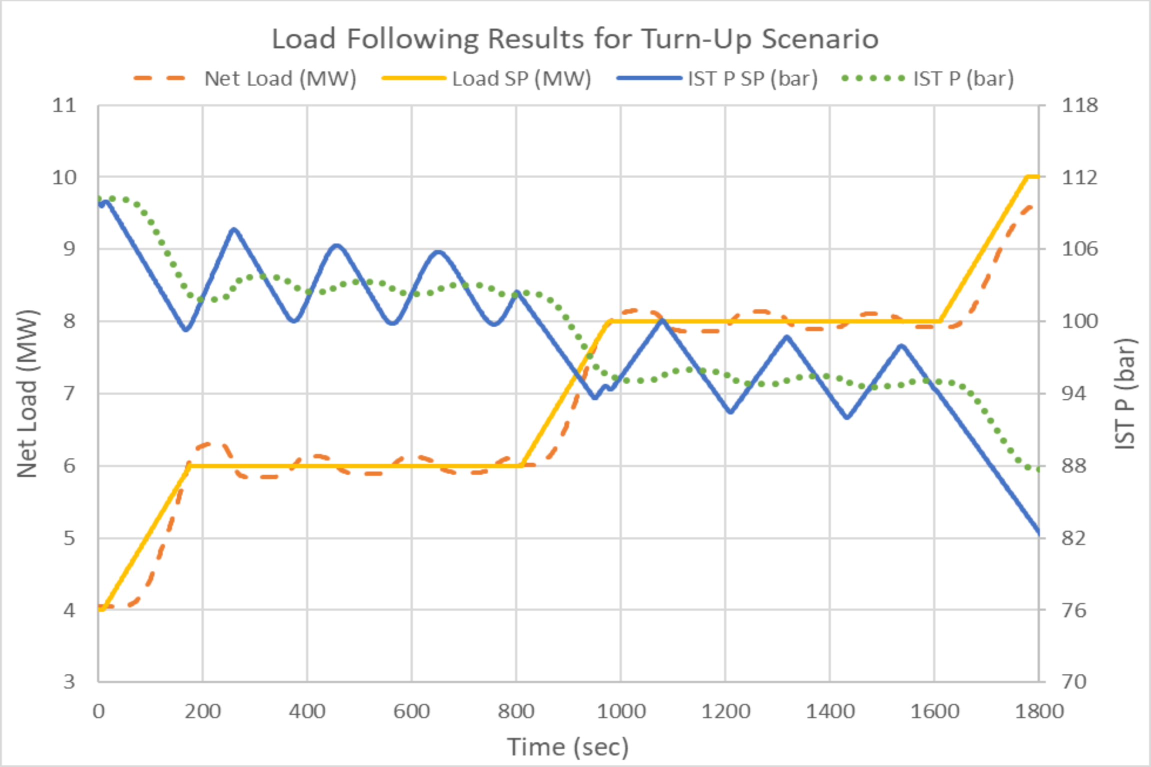

**Figure 5.** Load following response of MMPC to turn-up scenario

Table 2 summarizes the PV-SP average difference and settling time for each MPC for both the turn-up and turn-down scenario. As can be seen in Table 2, the avg. PV-SP difference and settling time for the turn-down scenarios are all improved over the previous work done in Albright et al. [6]. However, the majority of the cases for the turn-up response are worse, with the exception of $MPC_2$. The settling time for $MPC_3$ in the turn-up scenario was not recorded since the response did not reach the final demand SP. Overall, this data shows that there is promise to using this method within the $sCO_2$ RCBC but that there are still improvements that can be made, particularly to the turn-up response of this method.

**Table 2.** Load tracking difference and settling time for each method

| | Avg. Difference (MW) | Settling time, 2% of final SP (sec) |
|---|---|---|
| $MPC_1$, TD | 0.19 | 0 |
| $MPC_2$, TD | 0.062 | 0 |
| $MPC_3$, TD | 0.12 | 103 |
| $MPC_1$, TU | 0.39 | 255 |
| $MPC_2$, TU | 0.29 | 0 |
| $MPC_3$, TU | 0.43 | n/a |
| MWC [6], TD | 0.34 | 320 |
| MWC [6], TU | 0.37 | 196 |

## CONCLUSION

Advanced control techniques were applied to the $sCO_2$ RCBC in order to improve the load following response of the system. Improvements to the turndown response were achieved in the form of close load tracking and decreased settling time to fast ramps. The load following for the turn up scenario was not improved but does show that a multi-model approach may be important to improving separate sections of the controller response to this system. Additionally, a more centralized approach to the MPC may help to improve the performance by allowing the MPC to manipulate both the tank inlet and outlet valves independently.

This work shows that the $sCO_2$ RCBC has promising performance for fast ramps given strict control performance. Further enhancements to this control system can be made, including centralized MPC and adaptive MPC implementations.

## REFERENCES

[1] Marion J., Kutin M., McClung A., Mortzheim J., Ames R. The STEP 10 MWe $sCO_2$ pilot plant demonstration. In: ASME Turbo Expo, Phoenix, Arizona, 2019. https://doi.org/10.1115/GT2019-91917.

[2] Macadam S., Kutin M., Follett W.W., Subbaraman G. Supercritical $CO_2$ power cycle projects at GTI. In: European Supercritical $CO_2$ Conference, Paris, France, 2019. https://doi.org/10.17185/duepublico/48911.

[3] Marion J. Supercritical $CO_2$ 10 MW Demonstration Project Under Construction. Turbomachinery International, Vol. 63, No. 5, pp. 30-31, September/October 2022.

[4] Lesemann, M. “STEP Demo Team Pilots Innovative High-Efficiency Power Plant”. 27 Oct 2023. https://www.gti.energy/step-demo/step-demo-team-pilots-innovative-high-efficiency-power-plant/

[5] Liese E., Albright J., and Zitney S. “Startup, Shutdown, and Load Following Simulations of a 10 MWe Supercritical CO2 Recompression Closed Brayton Cycle”, J. of Applied Energy, Volume 277, 1 November 2020, 115628. https://doi.org/10.1016/j.apenergy.2020.115628

[6] Albright J., Liese E., Zitney S. “Control Methods for Mitigating Flow Oscillations in a Supercritical $CO_2$ Recompression Closed Brayton Cycle”, J. of Applied Energy, Volume 352, 15 Dec 2023, 121922. https://doi.org/10.1016/j.apenergy.2023.121922

## ACKNOWLEDGEMENTS

This work was performed in support of the US Department of Energy’s Fossil Energy and Carbon Management division. The research was executed through the NETL Research and Innovation Center’s Turbines program.

## DISCLAIMER